The Roy Griffiths Memorial Lecture paper

Acoustic remote sensing near the air-sea interface

D. M. Farmer

Institute of Ocean Sciences, 9860 West Saanich Road, Sidney, BC, V8L 4B2, Canada. farmerd@dfo-mpo.gc.ca

Abstract

At higher sea states the ocean surface layer presents some of the greatest challenges to observation. It is dynamic, imposes severe demands on in situ instrumentation and is subject to great variability over a wide range of space and time scales. Remote acoustical sensing can play a major role in resolving the physical properties of this environment, but the acoustical interpretations present interesting subtleties that must be understood before they can be used with confidence. Rather than attempt a summary of all the many new techniques being deployed in ocean surface research, this brief report focuses on a specific study directed at measurement of near surface velocities within wave crests so as to illustrate some of the challenges involved. Attenuation and scattering of the acoustical signal by bubble clouds is an important factor in setting limits to the range of conditions over which useful measurement can be achieved.

1. Introduction

At higher sea states acoustical remote sensing provides unique opportunities for observing the properties of wave breaking and related phenomena that defy measurement by traditional techniques. In this context acoustical methods fall into a few categories: the interpretation of naturally occurring sound, propagation measurements and back-scatter techniques such as Doppler measurement. While there are many naturally occurring sound sources in the oceans [1], a dominant contribution at higher sea states arises from breaking surface waves. Sound is radiated by air cavities as they deform and relax into spherical bubbles, providing a remote signal that is intimately related to the properties of the source mechanism. Breaking events can be tracked as they move across the ocean surface, providing a measure of their scale [2]. The radiated intensity appears to be correlated with quantity of air entrained, which in turn appears to be related to wave dissipation [3]. The energy dissipation associated with bubble break up is itself linked to the resulting bubble size distribution [4], and the size distribution of bubbles created in this process is related to the radiated sound spectrum.

In contrast to the interpretation of ambient sound, propagation measurements provide information on the medium through which the sound travels, especially inhomogeneities that scatter or refract the signal. Propagation is an essential aspect of active sonar measurement and in upper ocean research usually involves interaction with the surface and surface bubble clouds. Deane [5] reports separately on propagation measurements in the surf zone where multiple interactions with the surface and sea floor play a dominant role. Back-scatter measurement has proven especially effective in upper ocean studies at high sea states, due to the remarkable scattering properties of bubbles. Vertically oriented sonars pointing toward the surface detect not only the air-sea interface and hence the surface waves, but also bubble clouds injected by breaking waves and subsequently drawn deeper by the circulation. Horizontally scanning sonars provide striking images of bubble cloud organisation, especially that due to Langmuir circulation. Doppler processing of back scatter sonar signals provides information on upper ocean velocity fields, including the fine structure associated with wave breaking and Langmuir circulation, see summary and references in [6].

The present report summarises some recent studies of near surface velocity fields in the North Sea, in which obliquely incident sonar observations are used to measure the velocity field within the crests of large steep waves. Wave kinematics at high sea states is of great interest to the offshore engineering industry, for which accurate descriptions of wave loading are required for safe and economic design. Surface wave fields are routinely measured, but the distribution of wave forces imposed on a slender structure piercing the surface requires knowledge of the wave induced velocity field. The near surface wave velocity field can be reliably calculated for moderate waves, but the calculation becomes progressively less certain for large amplitude steep waves, especially when the waves are close to breaking. Indirect evidence points towards enhanced surface velocities in these conditions [7], but there is a need for accurate measurement in severe conditions.

A bistatic sonar was deployed for several months on the floor of the North Sea for this purpose. Our goal was to measure the three components of velocity right into the wave crests, so that wave loading could be calculated. Such measurements are ultimately limited by specular reflection of sidelobe energy from the surface. However, the way in which this specular reflection arises and the conditions under which the measurement becomes useful, depend on the character of the bubble field.

The following brief account draws attention to the subtle interplay between volume scattering by bubbles in the direct sonar path and attenuation by bubbles in obliquely incident surface scatter. Section 2.1 compares bubble population predictions from a recent theoretical model [4] with observations. Section 3 describes a bistatic measurement approach used in

TG Leighton, GJ Heald, HD Griffiths, G Griffiths, (eds.), 'Acoustical Oceanography', Proc. Institute of Acoustics Vol. 23 Part 2, 2001.

the North Sea. The bubble distributions described in Section 2.1 are then used to explain the limits imposed by specular reflection on near surface measurements. Preliminary results that confirm the analysis are presented in Section 4 along with a brief sample of surface elevation and velocity time series observations. A comprehensive analysis of results from the North Sea project, including comparison with different wave theories, will appear elsewhere [8].

2. Near surface bubble distributions

The importance of near surface bubbles as tracers of upper ocean circulation, as acoustical scatterers and as mechanisms for the enhancement of air-sea gas flux [9], have focused attention on improved methods of measurement. Single frequency sonars have been used with great success to measure bubble cloud distributions [9], but cannot measure bubble radius distributions. However, the high quality factor of bubbles at resonance ensures a strongly frequency dependent response, and some progress has been made with multiple frequency sonars [10], although difficulties arise from variability of sample volume with frequency. Moreover, attenuation can be severe leading to an ill-posed inversion. Thus size distribution measurement is better determined from *in situ* methods. Two quite different classes of acoustical measurement are in current use: nonlinear methods [11] and [12], and linear methods [13] and [14]. The important feature of such measurements is that they allow determination of the size distribution of bubbles as a function of time.

2.1 Bubble cloud dynamics

When a wave breaks, bubbles are formed across a wide radius range. The resulting distribution appears to approximate a power law over a fairly wide radius range, a physical process that has been explored in terms of its relationship to turbulent pressure fluctuations within the white cap [4]. This distribution evolves rapidly, however, and within seconds the bubble distribution properties have greatly changed. Bubbles injected beneath the surface are buoyant. Over a range of bubble radii (less than ~1000μm), larger bubbles rise faster than small ones, leading to a selective sorting of the size distribution within a bubble cloud, as illustrated in Figure 1. Bubbles also dissolve or grow, depending on the partial pressure differences of constituent gases across the bubble wall; turbulence and advection further redistribute the bubbles. Thus the size distribution of bubbles is a constantly evolving feature which provides insight on the near surface physics. Conversely, evaluation of acoustic scattering functions depends on a knowledge of bubble distributions.

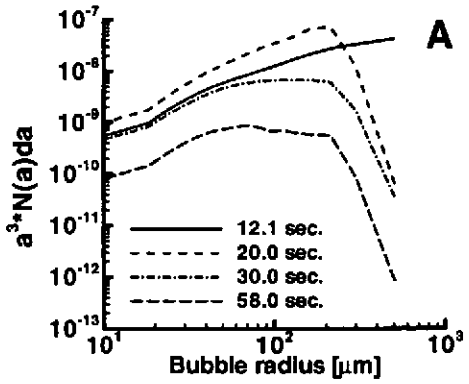

Figure 1. Measured bubble size distributions, shown with volume scaling, at successive intervals following a wave breaking event, (initial distribution identified as A) illustrating loss of larger bubbles through buoyancy sorting.

The link between acoustical properties and bubble dynamics can be illustrated with a simple model [4]. For a uniform initial bubble radius distribution, $N(a) = N_0 a^{-n}$, consider just two factors influencing the subsequent evolution: buoyancy and dissolution. The calculation neglects pressure effects and makes use of a simplification regarding effects of flow around the bubble on gas transfer, so that dissolution effects result in a constant rate of change in radius, $da/dt = -D$. The bubble rise rate is also assumed quadratic, $dz/dt \approx Aa^2$, which is a first order approximation for radii less than 500μm.. For bubbles initially injected uniformly over depth H, with periodicity T, the time averaged size distribution is

$$N(a,z) = \frac{N_0}{(1-n)BT}\left\{\left[a^3 + \frac{3B(H+z)}{A}\right]^{\frac{1-n}{3}} - a^{1-n}\right\}. \qquad (1)$$

This result illustrates the competition between buoyancy, which tends to remove the larger bubbles, and dissolution, which tends to decrease the radius of the smaller bubbles. For nominal values of $H = 2m$, $T = 60s$, $n = 3$, $A = 1.7\times10^{-6} m^{-1}s^{-1}$ and $D = (2z/H)\times10^{-4} m\cdot s^{-1}$, the balance is estimated to occur for $a \sim 100\mu m$, so that bubbles of approximately this size will contribute most to the air volume fraction in the bubble cloud and dominate the acoustical scattering and attenuation properties. Since a 100μm bubble resonates at a frequency of approximately 30kHz, acoustical attenuation and scattering is predicted to be maximal in this range. From Equation (1) we find that the spectral slope at large radii, for which dissolution is neglected, is a^{-2}, while at small radii, for which buoyancy can be neglected, the slope is a^{-5}. While there is much variability in the observed spectral slopes, they are of order of order -1.5 and -5 for small and large radii respectively. It is remarkable that such a simple model, which averages in time over many random breaking wave injections and omits all but the most basic physical processes, succeeds in capturing the essential character of the spectrum. The time averaged prediction (1) fails to account for the fact that bubbles are drawn down to much greater depths by Langmuir circulation [9, 15], but is a useful reference for comparison with observations.

Close to the surface, the decay of bubble concentration with depth is approximately exponential. We have acquired measurements of bubble size distributions at five depths over a range of wind speeds in the Gulf of Mexico. The measurements fit the following empirical time averaged relation:

$$N(a,z,W) = BW\exp(-z/D)p(a), \tag{2}$$

$$p(a) = \begin{cases} a^{-p_1} & a \le a_0 \\ \beta a^{-p_2} & a > a_0 \end{cases}, \tag{3}$$

where $N(a)$ is the number of bubbles per cubic meter per micron radius increment, W is wind speed at $10m$, and z is depth below the instantaneous ocean surface. The e-folding depth D is $0.7m$, but the reader should be cautioned that our shallowest measurement was $0.7m$. Consistent with the earlier result (1), we found that $a_0 = 100$ μm was appropriate for the data set, with $p_1 \sim 1.75$ and $p_2 \sim 5.0$. The parameter $\beta = a_0^{(p_2-p_1)}$ is adjusted to ensure continuity at a_o and $B = 4094$. This fit is a rather strong simplification. These are time averaged results, they neglect a tendency for a_o to decrease and for p_2 to increase with depth, but does provide a convenient representation for subsequent calculations of scattering and attenuation close to the surface.

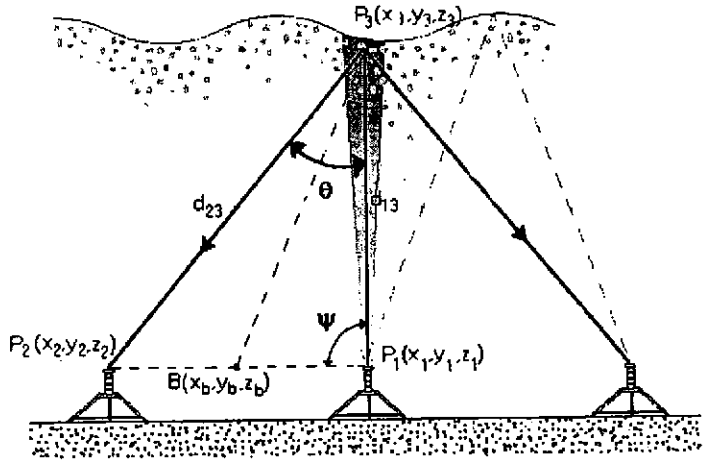

Figure 2. Bistatic sonar array. Three fan beam receivers (P_2) point in towards the beam of a single vertically oriented transmitter/receiver (P_1). Range gated signals detected at the four receivers are resolved into three components of velocity as a function of height. The triangular dashed path intersecting the surface to the right, represents the source of sidelobe specular scatter.

3. Bistatic measurements close to the ocean surface

Figure 2 is a sketch of the bistatic measurement array deployed at a depth of 40m in the North Sea [16]. A 100kHz coded pulse is transmitted vertically from a central circular transducer. The signal is scattered by bubbles within the water column and detected both as back scatter on the transmitting transducer and also obliquely on three fan-beam transducers. Doppler processing is used to calculate the three components of velocity as a function of depth, with the goal of resolving wave orbital velocities within the crests of large steep waves.

For the bistatic geometry used here, potential contamination by side-lobe surface scatter occurs at a depth of 2-3m beneath the sea surface directly above the transmitter. For the measurements to be useful, the magnitude of this surface scatter must be small relative to direct scatter from bubbles within the sample volume. The surface scatter is itself a function of sea state; however, the bubble density and penetration depth are also a function of sea state. Dense bubble clouds increase the magnitude of direct scatter from the sample volume, but also increase attenuation of the contaminating sidelobe acoustic path that must traverse the bubbles before and after intersecting the surface. The competition between these various effects must be evaluated to determine the wind speed range over which the measurements are meaningful.

Our calculation makes use of Kirchoff scattering theory [17] and the known transducer beam properties of the sonar. Generally, surface scattering intensity can be expressed as

$$< p_{ss}^{\,2} >= P_0^{\,2} R_0^{\,2} \frac{AS}{R_1^{\,2} R_2^{\,2}} b_2(\Theta_1, \Phi_1) \quad Att_1 , \tag{4}$$

where S is the surface scattering coefficient, A is the effective ensonified area on the surface, and R_1 and R_2 are the distances from the ensonified center to the transmitter and receiver respectively. The term $b_2(\Theta_1, \Phi_1)$ is the intensity directivity function of the receiver, and Att_1 is the attenuation factor. P_0 is the source pressure at range $R_0 = 1$m. It is assumed that there is no surface shadowing and that the ensonified area is small compared to R_1 and R_2. Following Medwin & Clay [17] we assume a Gaussian beam for the transmitter.

It can be shown that under the far-field assumption which is applicable here, when the acoustic roughness,

$$g = 4k^2 \sigma_h^{\,2} \cos^2 \theta_1 \tag{5}$$

is large, the specular scatter asymptotically approaches

$$S = C^2 / 16\pi\sigma_s^{\,2} , \tag{6}$$

where θ_1 is the incident angle, σ_h and σ_s are the RMS surface displacement and surface slope and C is the reflection coefficient for a perfectly smooth surface, taken as -1 in our application. Estimates [18] of the RMS surface slope lie within the range 0.17-0.26 for conditions corresponding to our data set.

The first sidelobe occurs at an angle of $\theta = 6^0$, but this angle is too small for specular reflections to be directed towards the obliquely oriented receivers. The most significant sidelobe occurs at $\theta = 15^0$, leading to potential interference in the sample volume lying ~3m beneath the surface. Although the obliquely oriented hydrophones do not point in the specular direction when the surface is flat, moderate surface slopes (~10^0) would be sufficient to direct specular reflections towards the hydrophones. The bistatic scattering intensity predicted by the Kirchoff model for this case may be expressed as

$$< p_{bi}^{\,2} >= P_0^{\,2} R_0^{\,2} Att_2 \frac{S_v \Delta R}{R_2'^2} \int b_1(\theta,\phi) b_2[\Theta(\theta,\phi), \Phi(\theta,\phi)] d\Omega \tag{7}$$

where P_0 is the source pressure at range $R_0 = 1$m, Att_2 is the attenuation factor which includes bubble effects, R'_2 is the distance from the bubble cloud center to the receiver, S_v is the volume scattering coefficient of bubbles, ΔR the vertical thickness of the ensonified volume in the bistatic setup, and b_1 ,b_2 are the intensity directivity functions of the source and receiving transducers. The receiving transducer beam angles Θ and Φ, are functions of the vertical and azimuthal angles θ and ϕ. Integration of (7) may be simplified by noting that the fan-beams are thin, allowing approximation by a narrow azimuthal window ($\delta\phi_0 = 2^0$).

The attenuation factor Att_2 for this path is dominated by the bubbles when these are present. For a given size distribution as a function of depth, the resulting extinction cross section $\alpha_e(x)$ may be integrated along the propagation path to find the excess attenuation associated with the bubbles:

$$P^2 = P_0^2 \exp\left\{-\int_0^L \alpha_e(l)dl\right\}. \tag{8}$$

The problem is rendered tractable under the simplifying assumption that the bubble distribution is horizontally homogenous, satisfying the general distribution given in (2) and (3).

4. Results

The relative sidelobe contribution may now be found as a function of wind speed. For the lowest sea state ($W = 7.3ms^{-1}$), the sidelobe reflection is 38 dB stronger than the bistatic scatter from bubble clouds, preventing any meaningful measurements of current velocity at 3m depth. At the highest measured sea state (W=17 ms^{-1}) however, the bistatic scatter is 21 dB stronger and sidelobe reflection will have little effect on the measured flow speed. These calculations imply a cross-over wind speed of 14-15 ms^{-1}; above 15 ms^{-1}, the sidelobe reflection rapidly becomes insignificant. From the perspective of evaluating wave kinematics in extreme conditions, the highest wind speeds are of greatest interest.

The validity of the above calculation may checked indirectly through comparison of velocity measurements using two different methods. The vertical velocity may be measured directly by Doppler analysis of the vertical beam. This measurement is free from any potential sidelobe scatter from the surface, since the range gating excludes surface reflections. Alternatively the vertical velocity may be derived from the obliquely detected signal on the three fan-beam transducers. A simple correlation analysis between these two methods will provide an indication of the relative significance of sidelobe contamination. Calculations were carried out at different depths over the available wind speed range. Velocity estimates using the two approaches are in close agreement at high sea states, but, as predicted, serious disagreement occurs at low sea states due to sidelobe contamination.

For the high wind speed example (W=17ms^{-1}), surface elevation and surface horizontal velocities are shown in Figure 3. Superimposed on the horizontal velocity time series is a prediction based on linear dispersion and the measured surface elevation. Small discrepancies arise because the calculation neglects wave spread, but extreme waves, such as that at $t = 288s$ typically illustrate significant underestimation by the linear theory. Comparisons with second and higher order Stokes' theory are a little closer, but still substantially beneath the measured values. The measured excess surface velocities are generally confined to the crests of large amplitude steep waves and provide an unambiguous record of enhanced surface flow that has long been suspected but not previously measured. In contrast, the discrepancies between observed and second order Stokes velocities at 3 m depth largely disappear. The Stokes model is also in close accord with observed velocities in the wave troughs.

5. Summary

Several acoustical methods have been developed for measurements of physical processes near the ocean surface. The acoustical properties of bubbles play a prominent role both in passive and active approaches, due to their high quality factor at resonance. An understanding of bubble dynamics is both aided by such measurements and also required in order to fully exploit the techniques. One particular example is used as an illustration: the application of bistatic Doppler sonar to the measurement of near surface velocities at high sea states. It is shown that the presence of bubbles is essential to the suppression of sidelobe contamination due to specular scatter. On the other hand, at the higher sea states of particular interest, excess attenuation of the specular path by bubbles effectively removes the contamination. The observations are generally in accord with model calculations, permitting finely resolved velocity measurement at and near the surface in the North Sea from an instrument placed on the sea floor.

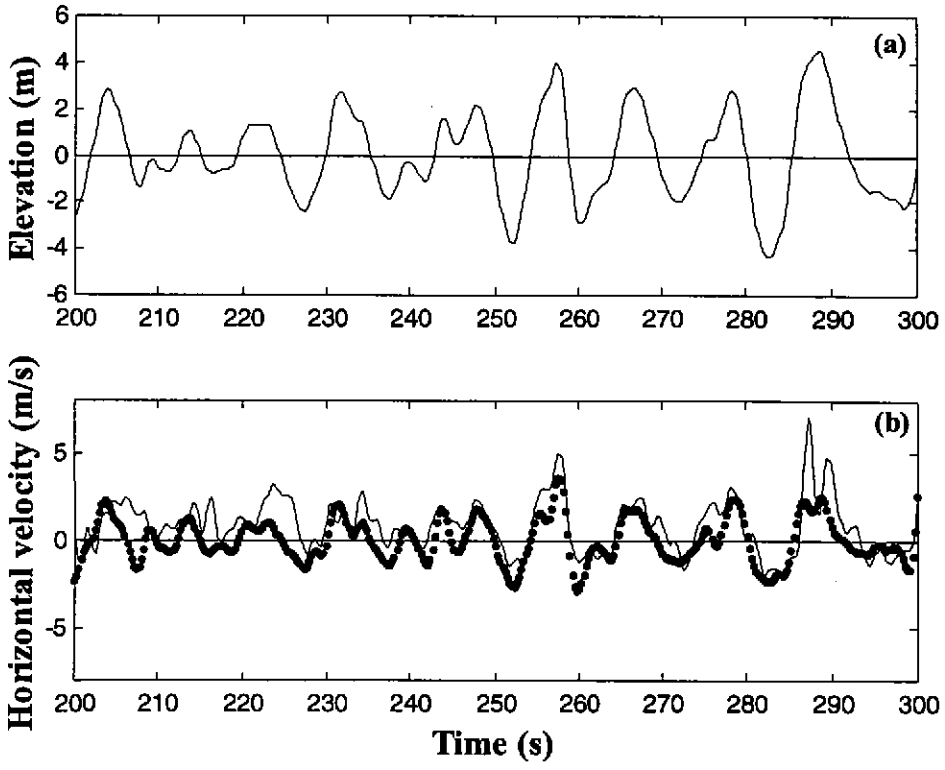

Figure 3. Sample time series of surface elevation above sonar and horizontal velocity component at the sea surface, resolved in dominant wave direction. Dotted line shows prediction by irregular linear theory. Note discrepancy at ~288s.

6. Acknowledgement

The work described here was part of a collaborative study involving colleagues at LIC Engineering A/S, A D Booth and L Ding.

7. References

[1] Buckingham M, and Potter JR, Sea Surface Sound '94, *Proceedings of the III International Meeting on Natural Physical Processes Related to sea Surface Sound,* University of California, Lake Arrowhead, 7 - 11 March 1994, World Scientific Publishing Co.

[2] Ding L and Farmer DM. Observations of breaking surface wave statistics. *J. Phys. Oceanogr.*, 1994; **24**(6): 1368-1387.

[3] Melville WK, Loewen MR, Felizardo FC, Jessup AT and Buckingham MJ. The Acoustic and Microwave Signatures of Breaking Waves. *Nature*, 1988; **336**, 54-56.

[4] Garrett C, Li M and Farmer DM. The Connection Between Bubble Size Spectra and Energy Dissipation Rates in the Upper Ocean. *J. Phys. Oceanogr.*, 2000; **30**: 2163-2171.

[5] Deane G. Acoustical Oceanography in the Coastal Environment, in *'Acoustical Oceanography', Proceedings of the Institute of Acoustics Vol. 23 Part 2, 2001,* T G Leighton, G J Heald , H Griffiths and G Griffiths, (eds.), Institute of Acoustics, (this volume), pp. 308-214.

[6] Farmer DM. Observing the Ocean Side of the Air-Sea Interface. *Oceanography*, 1997; **10**(3): 106-110.

[7] Sand SE *et al.* Freak Wave kinematics. Advanced Research Workshop Water Wave Kinematics, Molde, Norway, May 1989.

[8] Farmer DM, Ding L, Booth D, and Lohmann M. Wave Kinematics at high sea states, to appear in *J. Atmosph. & Ocean. Technology* 2001

[9] Thorpe SA. On the clouds of bubbles formed by breaking wind-waves in deep water, and their role in air-sea gas transfer. *Philos.Trans.Roy.Soc.London* A, 1982; **304**: 155-210.

[10] Vagle S and Farmer DM. The measurement of bubble size distributions by acoustical backscatter, *J. Atmosph. & Ocean. Technology*, 1992; **9**(5): 630-644.

[11] Leighton TG, Meers SD, Simpson MD, Clarke JWL, Yim GT, Birkin PR, Watson Y, White PR, Heald GJ, Dumbrell HA, Culver R L and Richards SD. The Hurst Spit experiment: The characterisation of bubbles in the surf zone using multiple acoustic techniques, in *'Acoustical Oceanography', Proceedings of the Institute of Acoustics Vol. 23 Part 2, 2001,* T G Leighton, G J Heald , H Griffiths and G Griffiths, (eds.), Institute of Acoustics, (this volume), pp. 227-234.

[12] Didenkulov IN, Muyakshin SI and Selivanovsky DA. Bubble counting in the subsurface ocean layer, in in *'Acoustical Oceanography', Proceedings of the Institute of Acoustics Vol. 23 Part 2, 2001,* T G Leighton, G J Heald , H Griffiths and G Griffiths, (eds.), Institute of Acoustics, (this volume), pp. 220-226.

[13] Farmer DM, Vagle S and Booth AD. A free-flooding acoustical resonator for measurement of bubble size distributions, *J. Atmos. & Oceanic Technol.*, 1998; **15**(5): 1132-1146.

[14] Terrill EJ and Melville WK. A broadband acoustic technique for measuring bubble size distributions: laboratory and shallow water measurement. *J. Atmos. & Oceanic Technol.*, 2000; **17**: 220-239.

[15] Farmer DM, Vagle S and Li M. Wave breaking, turbulence and bubble distributions in the ocean surface layer. Air-Sea Symposium, 1999, Sydney, Australia.

[16] Farmer DM, Ding L, Booth AD and Lohmann M. Wave kinematics at high sea states, 2001, *to appear, J. Atmos. & Oceanic Engineer.*

[17] Medwin H, and Clay CS. Fundamentals of Acoustical Oceanography, Academic Press 1998

[18] Cox CS and Munk W. Statistics of the Sea Surface Derived from Sun Glitter. *J. Mar. Res.*, 1954; **13**: 198-227.